Cluster-weighted percolation-a novel approach to the Potts model

Cluster-weighted percolation—a novel approach to the Potts model

Thomas A Larsson

Department of Theoretical Physics, Royal Institute of Technology, S-100 44 Stockholm, Sweden

Abstract. The random-cluster expansion of the n-state Potts model can be understood as an interacting percolation problem: 'cluster-weighted bond percolation'. This interpretation explains the phase transition in the Potts model as a percolation transition, and it also suggests several generalisations. We employ a position space renormalisation group to calculate the transition temperature and the critical exponents.

1. Introduction

It is well known that the partition function of the n-state Potts model can be expanded in a sum over all possible graphs on the lattice (see Wu 1982 and references therein):

$$Z = \sum_{\text{configs}} n^c u^b \tag{1.1}$$

where b is the number of occupied bonds and c is the number of clusters in the graph. Kasteleyn and Fortuin (1969) found that (1.1) describes bond percolation in the $n \to 1$ limit. In this paper we consider (1.1) for arbitrary n from the point of view that it describes an interacting percolation problem. Since the difference from ordinary bond percolation is that each cluster has acquired a fugacity n, we propose to name this problem 'cluster-weighted (cw) bond percolation'. The reason for introducing a new name for this particular form of the old Potts model is threefold. First, the name emphasises that we are dealing with a percolation problem, which is characterised by some percolation threshold, some connectedness length, an infinite fractal cluster, etc. We will show in § 2 that all these aspects of cw percolation are intimately related to the critical behaviour of the Potts model, just as they are when $n = 1$. This point of view does not lead to any new knowledge in itself, but it may offer new insights into the old problem.

Second, the graph expansion can be generalised in a number of ways which are not obvious from the Potts model. Some of these variations may not even possess a Hamiltonian formulation. One such generalisation, cw site percolation, is considered in this paper.

Third and finally, the cw percolation problem is amenable to treatment with renormalisation group (RG) tools, developed for percolation and similar problems. Most RG methods rely on the existence of a Hamiltonian formulation of the problem. This is true in particular for field-theoretic methods (Priest and Lubensky 1976, Amit 1976), the Migdal–Kadanoff RG (Migdal 1976, Kadanoff 1976, Andelman

and Berker 1981), etc. One of the major advantages of the connection between percolation and the Potts model has been that these tools have been available for percolation as well. On the other hand, Reynolds *et al* (1977, 1978) have devised a position space RG (PSRG) for percolation directly, without reference to the Potts model. This PSRG method has been reviewed by Stanley *et al* (1982). It has become very popular because of its conceptual simplicity, and also because it is capable of producing quite accurate numbers. In § 3 we show how to extend this method to treat CW percolation, and thus also the Potts model. This is the main objective in this paper. Finally, in § 4 we discuss the feasibility of this approach and a number of generalisations.

2. Aspects of CW percolation

2.1. Equivalence between 'cluster-weighted percolation' and the n-state Potts model

Consider an n-state Potts model in a magnetic field on an arbitrary lattice. The negative of the Hamiltonian, in units of $k_B T$, is

$$-\mathcal{H} = \sum_{\langle ij \rangle} J\delta_{\sigma_i,\sigma_j} + \sum_i h\delta_{\sigma_i,1}. \tag{2.1}$$

The partition function can be expanded in a sum over all possible graphs on this lattice:

$$Z \equiv \mathop{\text{Tr}}_{\{\sigma\}} \exp(-\mathcal{H}) = \sum_{\text{configs}} u^b \prod_c [\exp(hs_c) + n - 1] \tag{2.2}$$

where b is the number of occupied bonds, $u = \exp(J) - 1$ is the weight of such a bond, and s_c is the number of sites in the cluster c. The unoccupied links are given a fugacity of one. This is of course purely conventional. Indeed, with $x = uy$ and y arbitrary, Z can be rewritten as

$$Z = y^{-N} \sum_{\text{configs}} x^b y^{N-b} \prod_c [\exp(hs_c) + n - 1]. \tag{2.3}$$

In (2.3), x is the fugacity of occupied bonds and y is the fugacity of empty ones. In ordinary percolation, it is convenient to choose $y = 1 - x$, so x can be interpreted as the occupation probability of a bond. However, in this section we will adhere to the notation in (2.2). Following Wu (1982), we can now introduce

$$G_n(J, h) \equiv N^{-1}\frac{\partial}{\partial n} \ln Z = N^{-1} \sum_c \langle [\exp(hs_c) + n - 1]^{-1} \rangle. \tag{2.4}$$

Clearly, in the limit $n \to 1$, (2.4) reduces to

$$G_1(J, h) = N^{-1} \sum_c \langle \exp(-hs_c) \rangle \tag{2.5}$$

from which we can deduce the quantities of interest in percolation. However, we can also consider derivatives of G_n with respect to h for arbitrary n, e.g.

$$G_n'(J, h) = -N^{-1} \sum_c \frac{\langle s_c \rangle}{n^2} \equiv (P_n(u) - 1)/n^2. \tag{2.6a}$$

$$G_n''(J, h) = N^{-1} \sum_c \frac{2-n}{n^2}\langle s_c^2 \rangle \equiv \frac{2-n}{n^2} S_n(u). \tag{2.6b}$$

$P_n(u)$ and $S_n(u)$ are the generalisations of the corresponding quantities in ordinary percolation, i.e. P_n is the probability of a site chosen at random to belong to the infinite cluster, and S_n is the mean cluster size. Their singularities are determined by the Potts critical exponents β and γ, respectively, which is obvious from their definition in terms of the Potts model. More interestingly, the critical coupling of the Potts model corresponds exactly to the percolation weight of cw bond percolation, $u_c = \exp(J_c) - 1$. This is easily seen from (2.6). The probability of belonging to the infinite cluster and the spontaneous magnetisation are singular simultaneously. Also, the mean cluster size diverges when the Potts susceptibility does so. This implies that, provided there is only one critical point in the Potts model, it must be connected with the appearance of an infinite cluster in the diagrammatical expansion.

2.2. Fractal dimensionality of the infinite cluster

We can further exploit the percolation analogy to find a geometrical interpretation of the magnetic scaling power y_h. In terms of the usual critical exponents, $y_h = (\beta + \gamma)/\nu$. In the $n = 1$ case, y_h is known to equal the fractal dimensionality of the incipient infinite of ordinary percolation (Stanley 1977, Kirkpatrick 1978, Stanley and Coniglio 1983—the standard text on fractals is Mandelbrot (1982)). Analogously, the magnetic exponent of the n-state Potts model may be interpreted as the fractal dimension of the infinite cluster in the corresponding cw percolation problem.

Before we show this, we first need to generate a typical cw percolation graph. This is not as easy as in ordinary percolation, because of the long-range interaction caused by the cluster fugacity. Instead, we can imagine a two-step process.

(1) Generate all possible graphs on the (finite but large) lattice. To every graph we assign a weight $u^b n^c$.

(2) Pick a graph at random from this sample, with a probability proportional to its weight. If $u = u_c$, the typical configuration so generated has large clusters characterised by a fractal dimensionality y_h, which we now proceed to show. To this end, we can copy the arguments of Stanley and Coniglio (1983) more or less *verbatim*.

We assume the usual scaling ansatz for the singular part of the generating function G_n of (2.4):

$$G_n(\varepsilon, h) = \lambda^{-d} G_n(\lambda^{y_t}\varepsilon, \lambda^{y_h} h) \tag{2.7}$$

where

$$\varepsilon = \left|\frac{J - J_c}{J_c}\right| = \left|\frac{u - u_c}{u_c}\right|.$$

Choose rescaling factor so that $\lambda^{y_t}\varepsilon = 1$. Then

$$G_n(\varepsilon, h)/\varepsilon^{d/y_t} = G_n(1, \varepsilon^{-y_h/y_t}h) \equiv f(s^*h). \tag{2.8}$$

Here the variable $s^* = \varepsilon^{-y_h/y_t}$, which is conjugate to the magnetic field h, will be interpreted as a typical size of scaling clusters. Since the only relevant length scale in the problem is the correlation length ξ, it must be the linear dimension of the largest clusters present. Since the correlation length is proportional to ε^{-1/y_t} close to criticality, we have

$$\varepsilon^{-y_h/y_t} = s^* \propto \xi^D \propto (\varepsilon^{-1/y_t})^D. \tag{2.9}$$

From this relation it immediately follows that $D = y_h$.

2.3. CW *percolation versus 'droplets'*

CW percolation gives a tangible geometrical interpretation of the magnetic scaling power y_h for arbitrary n. A different formulation was put forward by Coniglio and Klein (1980). They considered 'droplets' in the Ising model. These droplets are constructed from adjacent up spins, connected by 'active bonds', each bond being 'active' with probability $p_B = 1 - \exp(-2J_{Ising})$. The idea behind this is to remove the superficial correlations that are already present at infinite temperatures. J_{Ising} is the coupling constant in the Ising model. In terms of the Potts interaction strength J, $J_{Ising} = J/2$. Therefore, the activation probability can be expressed as $p_B = 1 - \exp(-J)$, which means that p_B satisfies the equation

$$p_B = u(1 - p_B) \tag{2.10}$$

where u is the weight of a bond in CW percolation.

This similarity leads us to suspect that there is some close connection between CW percolation and the droplet picture. Indeed, droplets can be viewed as a simulation of a typical term in the graph expansion. To show this, we recall that the partition function can be written as

$$Z = \mathop{\mathrm{Tr}}_{\{\sigma\}} \prod_{\langle ij \rangle} [u\delta_{\sigma_i\sigma_j} + (1 - \delta_{\sigma_i\sigma_j})]$$

$$= (1 - p_B)^{-N} \mathop{\mathrm{Tr}}_{\{\sigma\}} \prod_{\langle ij \rangle} [p_B\delta_{\sigma_i\sigma_j} + (1 - p_B)(1 - \delta_{\sigma_i\sigma_j})]. \tag{2.11}$$

If we view this expression as a recipe to simulate the graph expansion, p_B is the probability of putting a bond between two neighbours, while the trace over spins is simulated by thermal equilibrium. But this is exactly what the Coniglio–Klein droplets are doing. Hence, it is not surprising that they have the same fractal dimension as the infinite percolation cluster in the graph expansion.

To use droplets is probably the only viable way to attack CW percolation with direct simulation. In contrast, the exact enumeration method outlined in the previous subsection is totally inadequate for practical purposes, although it gives a conceptual basis.

2.4. *Cluster-weighted site percolation*

Apart from being a convenient setting for the interpretation of the magnetic scaling power in the Potts model, the diagrammatical expansion also suggests some new generalisations. One such generalisation of the Potts model is 'cluster-weighted site percolation'. This problem can be defined by a partition function

$$Z = \sum_{\text{configs}} u^s n^c. \tag{2.12}$$

Here the basic quantities which might be occupied or not are the sites of a regular lattice; s is the number of such occupied sites in the configuration and c is the cluster number. Two sites are defined as belonging to the same cluster if there is a path of adjacent occupied sites which joins them. Ordinary site and bond percolation, with $n = 1$, are believed to belong to the same universality class. This is not true for the CW counterparts with the same $n \neq 1$, due to different ways of counting clusters. In particular, the $n \to 0$ limit of (2.12) is the generating function for site lattice animals (differentiate (2.12) with respect to n, and only configurations with one cluster survive in this limit), while the $n \to 0$ limit of (1.1) describes the statistics of spanning trees

(Wu 1982). On the other hand, we believe that a modified form of cw bond percolation will lie in the same universality class as (2.12). This modified problem is also described by the partition function (1.1), but c now stands for the number of 'bond clusters', i.e. clusters containing at least one occupied bond. Hence, isolated sites are not considered to be clusters in this model. We will refer to the modified problem as cw bond percolation of type II, while the Potts model gives rise to type I cw bond percolation. The $n \to 0$ limit of the type II model describes the statistics of bond lattice animals, so at least when $n = 0$ and $n = 1$ this model should have the same critical behaviour as the site version.

3. Position space renormalisation group

We now want to apply psrg techniques to calculate critical exponents for cw percolation. Previously, most rg calculations have been concerned with the Hamiltonian formulation of the problem; this is particularly true for field-theoretical methods. On the other hand, Reynolds *et al* (1977, 1978) have developed a very physical large-cell rg for percolation, without reference to the Potts model. We extend this method to treat type I cw bond percolation, and thus also the n-state Potts model.

First we redefine the partition function (1.1) so that only the singular part remains:

$$Z = \sum_{\text{configs}} n^c x^b y^{N-b}. \tag{3.1}$$

Thus, compared to (2.3), an analytic factor has been dropped. Now consider a $\lambda \times \lambda$ cell, like the one in figure 1. We generate all possible configurations of b occupied and $N - b$ empty bonds on this cell, and give each configuration a weight according to (3.1). Here $N = 2\lambda^2 - \lambda$ is the total number of links in the cell (the λ links on the extreme right were discarded, since they do not affect the percolation property of the configuration) and c is the cluster number. In calculating c, one should keep in mind

(a)

(b)
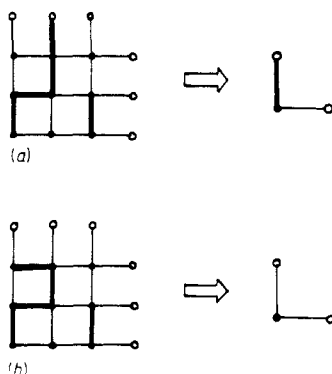
Figure 1. (*a*) A typical percolating configuration of a 3×3 cell. This graph gives a contribution to the sum in (1.1) with $b = 5$ and $c = 5$. (*b*) A typical non-percolating configuration. $b = 5$ and $c = 4$. In type II cw bond percolation, introduced at the end of § 2, the number of clusters is altered to $c = 2$ in both *a* and *b*. The number of percolating sites, as well as percolating bonds, is 4 in *a*. Note that the open circles belong to adjacent cells.

that the open circles in figure 1 belong to adjacent cells, and hence they should not be counted. The renormalised weights are then defined by

$$nx' = \sum_{\substack{\text{percolating} \\ \text{configs}}} n^c x^b y^{N-b} \equiv R_\lambda(x, y) \tag{3.2a}$$

$$ny' = \sum_{\substack{\text{not percolating} \\ \text{configs}}} n^c x^b y^{N-b} \equiv Q_\lambda(x, y) \tag{3.2b}$$

where a configuration is considered to percolate if there is at least one path that connects the upper and lower boundaries of the cell. Of course, alternative definitions of 'percolating' are conceivable, but in the infinite-cell limit they should all be equivalent. It should be noted that we consider the cluster weight n to be a parameter rather than a variable, so n is left unchanged by the RG transformation. This is in accordance with the experience that the Potts model for each n has different exponents, and hence there is one fixed point for each n.

Explicitly, in the case $\lambda = 2$, the right-hand members of (3.2) become

$$R_2(x, y) = n(8x^4 y^2 + 6x^5 y + x^6) + n^2(8x^3 y^4 + 5x^4 y^2) + n^3(2x^2 y^4 + 2x^3 y^3) \tag{3.3a}$$

$$Q_2(x, y) = n(4x^3 y^3 + x^4 y^2) + n^2(6x^2 y^4 + 4x^3 y^3 + x^4 y^2)$$
$$+ n^3(4xy^5 + 6x^2 y^4 + 2x^3 y^3) + n^4(y^6 + 2xy^5 + x^2 y^4). \tag{3.3b}$$

If we set $x = 1 - y = p$ and $n = 1$, (3.3a) reduces to (12) of Reynolds *et al* (1977).

We performed RG transformations from cells of linear size two and three, as well as a cell-to-cell transformation from $\lambda = 3$ to $\lambda = 2$. Subsequently, we will denote an RG transformation from a cell of size λ_2 to a cell of size $\lambda_1 < \lambda_2$ by a 'λ_2/λ_1 transformation'. In particular, cell-to-bond transformations have $\lambda_1 = 1$.

The critical fugacity and the thermal scaling power follow as usual from the recursion relation (3.2). In figure 2, we show how the location of the critical fixed point (x^*, y^*), from the 3/2 transformation depends on n. For all n, there is also a dilute fixed point at $(x, y) = (0, 1)$, a low-temperature fixed point at $(1, 0)$ and an additional, stable,
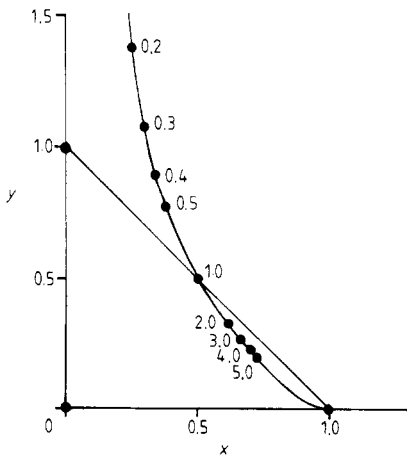

Figure 2. Critical fixed points in the xy plane for CW bond percolation, obtained from a 3/2 transformation. The fixed points $(1, 0)$, $(0, 1)$ and $(0, 0)$ are also indicated, as well as the line $y = 1 - x$. Note that the critical fixed point only lies on this line when $n = 1$.

fixed point in the origin. It is interesting to observe that when $n = 1$ the RG picks out a fixed point on the line $y = 1 - x$. Therefore it is natural to identify x with the occupation probability in the special case. For other values of n, such an interpretation is incorrect.

It is not necessary to consider a two-parameter RG. In fact, dividing (3.2a) by (3.2b), we find the following recursion relation for the variable $u = x/y$:

$$u' = R_\lambda(u, 1)/Q_\lambda(u, 1). \tag{3.4}$$

In figure 3, we have plotted the fixed point $u^* = x^*/y^*$ as a function of n. The results are compared to the exactly known critical point of the Potts model on a square lattice, $u_c = \sqrt{n}$ (Wu 1982). When $n = 1$, the exact value $u_c = 1$ is reproduced by duality. For other n the agreement is not very good, and especially the non-analyticity at $n = 0$ is not obtained by the RG. However, the 3/2 transformation yields a clear improvement over the 2/1 transformation, indicating that larger cells produce better results.
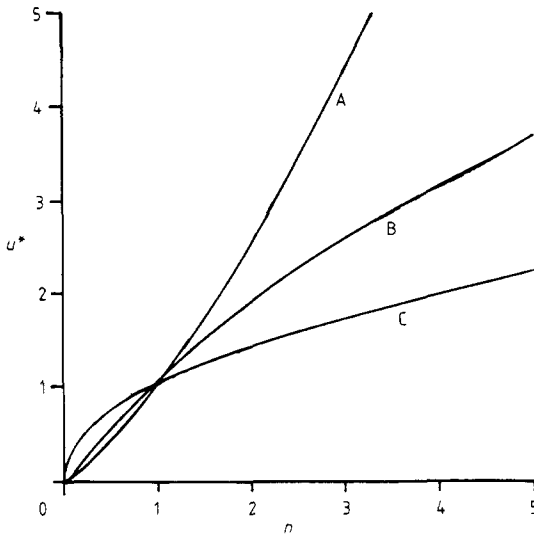
Figure 3. Fixed point $u^* = x^*/y^*$ for CW bond percolation. Curve A: 2/1 transformation. Curve B: 3/2 transformation. Curve C: exact.

Because we have constructed a two-parameter RG, there will be two thermal eigenvalue exponents. The minor of these we identify with the thermal exponent of the Potts model, $y_t = \nu^{-1}$; this is also precisely the same exponent as the one-parameter RG (3.4) yields. The major exponent turns out to be independent of n. Specifically, the latter exponent equals $\ln 6/\ln 2 = 2.5850$, $\ln 15/\ln 3 = 2.4650$, and $\ln \frac{5}{2}/\ln \frac{3}{2} = 2.2599$, for 2/1, 3/1 and 3/2 transformations respectively. y_t is plotted as a function of n in figure 4. Again, comparison with the exact result is not favourable except in an intermediate regime, but larger cells produce better results. Also, we found no signs of the first-order transition above $n = 4$, although y_t kept increasing with n.

We now proceed to obtain the magnetic scaling power, which by § 2 equals the fractal dimensionality D of the critical percolation cluster. One of the main properties of D is that it determines the mass of a cluster within a region of linear dimension R. In the PSRG approach, we can tentatively identify R with the cell size λ. If we then
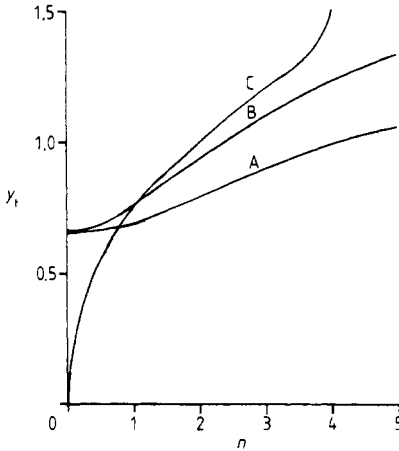
Figure 4. Thermal exponent $y_t = \nu^{-1}$. Curve A: 2/1 transformation. Curve B: 3/2 transformation. Curve C: exact.

assign unit mass to each site in the percolating cluster(s), we have

$$\langle s \rangle_\lambda \equiv \sum_{\substack{\text{percolating} \\ \text{configs}}} sn^c x^b y^{N-b} \left(\sum_{\substack{\text{percolating} \\ \text{configs}}} n^c x^b y^{N-b} \right)^{-1} \propto \lambda^D \tag{3.5}$$

where s is the number of sites in the percolating cluster, and the sum only encompasses percolating configurations. The expression is evaluated at the fixed point. Note that the denominator in (3.5) equals the renormalised weight x', and thus also x at the fixed point. Introducing the function

$$S_\lambda(x, y) \equiv \sum_{\substack{\text{percolating} \\ \text{configs}}} sn^c x^b y^{N-b} \tag{3.6}$$

our estimate for the fractal dimension follows from

$$\left(\frac{\lambda_2}{\lambda_1} \right)^D = \frac{S_{\lambda_2}(x^*, y^*)}{S_{\lambda_1}(x^*, y^*)}. \tag{3.7}$$

One can easily convince oneself that $S_1(x, y) = nx$, while we find the following explicit expression when $n = 2$:

$$S_2(x, y) = n(32x^4y^2 + 24x^5y + 4x^6) + n^2(22x^3y^3 + 16x^4y^2) + n^3(4x^2y^4 + 4x^3y^3). \tag{3.8}$$

The fractal dimensionalities from 2/1 and 3/2 transformations are plotted in figure 5, together with the exact Potts result. Again, the agreement is not particularly good, but it improves with increasing cell size. Also, poor agreement for small n is to be expected, since the approximate fixed point deviates strongly from the exact one in this range.

    Of course, we could have assigned unit weight to each *bond* of the spanning cluster instead, with essentially the same result, at least in the infinite-cell limit. However, to do this properly, we would also have had to account for the extreme-right bonds in figure 1, which would increase computing time (and cost!) with a factor 2^λ. Tentatively, we counted the number of bonds neglecting the rightmost ones, which yielded approximately the same results as did (3.7) for small n, while the estimate for large n exceeded two.
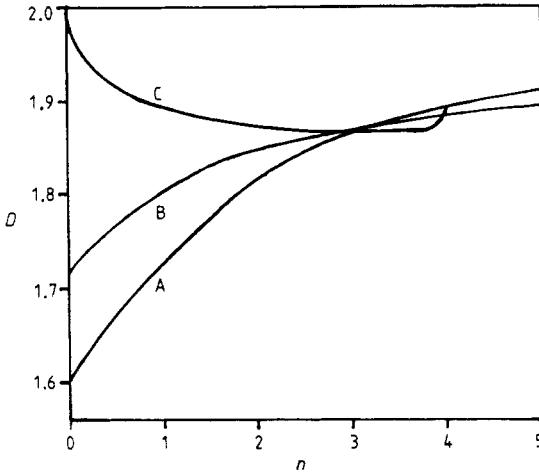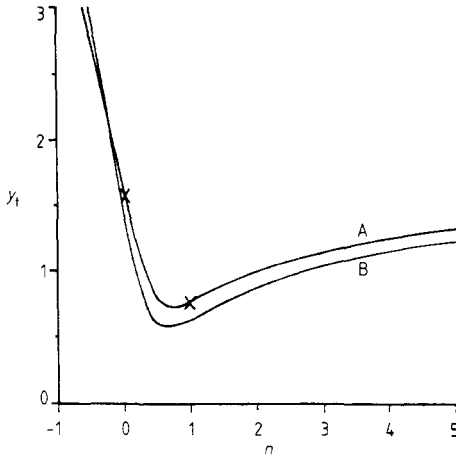
Figure 5. Fractal dimensionality D of the percolating cluster in CW bond percolation. Curve A: 2/1 transformation. Curve B: 3/2 transformation. Curve C: exact magnetic eigenvalue exponent.

Finally, we also attempted to introduce 'ghost' bonds *à la* Reynolds *et al* (1977). For the small cells we used in our calculations, the resulting eigenvalue exponent exceeded two for small and intermediate n, including $n = 1$, which of course is not acceptable. Also in this case we observed an improvement with increasing cell size, however.

We also attacked CW site percolation and type II CW bond percolation with the same PSRG approach. In this case we do not have an exact solution to compare with, except that we know the critical exponents for $n = 1$ and that $y_t \approx 1.56$ for $n = 0$ (lattice animal limit, Derrida and de Sèze 1982). The calculations followed the same tracks as previously. Our best results are presented in figures 6-8. A comparison between the curves in figures 7 and 8 clearly indicates that both models belong to the same
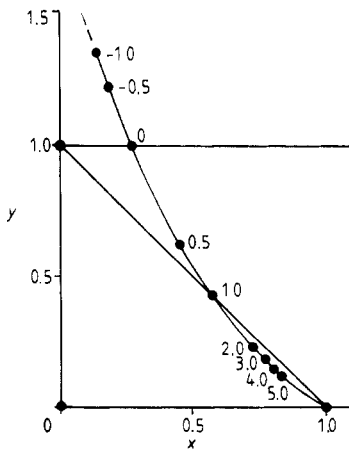
Figure 6. Critical fixed point in xy plane for CW site percolation, from 4/3 transformation, for some value of the parameter n. Fixed points at $(0, 1)$, $(1, 0)$ and $(0, 0)$ are also present. Note that the critical fixed point intersects the line $y = 1 - x$ at $n = 1$, and the line $y = 1$ at $n = 0$.

Figure 7. Thermal exponent y_t for CW site percolation and type II CW bond percolation. Curve A: type II bond, 3/2 transformation. Curve B: site, 4/3 transformation. The crosses indicate exact values.
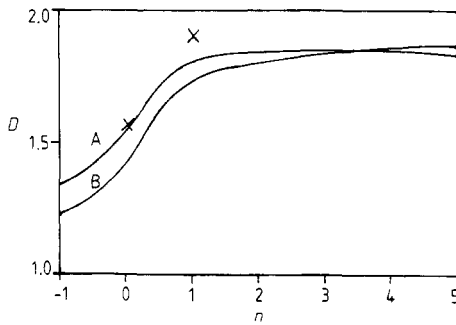
Figure 8. Fractal dimensionality D of the critical cluster. Curve A: type II CW bond percolation, 3/2 transformation. Curve B: CW site percolation, 4/3 transformation. The crosses indicate exact values.

universality class, as anticipated in § 2. It is reassuring to observe that the fixed point is again located on the line $y = 1 - x$ when $n = 1$, and also that it lies on $y \equiv 1$ when $n = 0$. We extended our investigation some distance into the region of negative n. Although this perhaps is somewhat artificial, fixed points and critical exponents behaved smoothly, at least within our PSRG. It is notable that the thermal eigenvalue exceeds two for $n \leqslant -0.19$.

4. Discussion

We have shown how the phase transition in the Potts model may be interpreted as the appearance of an infinite cluster in the graph expansion, and also that the magnetic scaling power has an attractive interpretation as a fractal dimensionality of this infinite cluster. The very concrete geometric approach to the phase transition which is offered by the 'cluster-weighted percolation' picture is likely to increase our understanding of

the phase transition in the Potts model, and of critical phenomena in general. For example, we know that the n-vector model can be expanded in graphs consisting of all possible closed loops. In analogy with CW percolation, we expect that the phase transition in this model is accompanied by the appearance of an infinite loop.

Recently, much attention has been given to fractal properties of percolation clusters. One can identify the analogous fractal sets for CW percolation as well and ask the same questions, e.g. 'Do the Alexander-Orbach (1982) or the Aharony-Stauffer (1984) conjectures hold?'; 'Is the fractal dimension of the "red" bonds equal to the thermal scaling power of the corresponding Potts model (Coniglio 1982)?'; 'Are there any scaling relations between these fractal dimensionalities (Stanley 1984)?', etc. We believe that it is important to have more models to investigate to see if the various conjectures are limited to ordinary percolation or if they have a broader scope. CW percolation may play the role of one such 'testing ground', since at least type I CW percolation with $n = 2$ and $n = 3$ should be amenable to a Monte Carlo simulation of Coniglio-Klein (1980) droplets.

The graphical expansion was originally devised as a method to calculate high-temperature series. At high temperatures, the partition function is dominated by diagrams with few occupied links, and hence it is easy to calculate. At low temperatures, on the other hand, the partition function is also easy to express as an expansion in the number of empty bonds. But at the critical point the important diagrams are those with about as many occupied as empty links. This class of diagrams is huge, containing diagrams of all sizes and shapes, without any natural cut-off. But it is precisely such problems in which the RG approach is appropriate. In § 3 we showed how to perform a PSRG calculation on CW percolation. The results were qualitatively acceptable in an intermediate range, while our method ran into difficulties close to the non-analyticities at $n = 0$ (fixed point $= \sqrt{n}$) and $n = 4$ (transition to first-order behaviour). For CW site and type II CW bond percolation we apparently do not have any such problems; at least the fixed point behaves smoothly for all interesting n. An eventual first-order transition would probably not be detected in this case either. An interesting observation is that the bond variant comes much closer to the exactly known exponents. As a matter of fact, the thermal scaling power from the bond 3/2 transformation lands almost right onto the crosses in figure 7, in spite of the smallness of the cells. We cannot offer any explanation for this difference in performance, but only note its existence.

One would think that the accuracy of the PSRG would be greatly enhanced if it were combined with a Monte Carlo simulation of the configurations in (3.2). However, some thought (combined with a failing attempt) indicates that this is not the case, except close to $n = 1$. The reason for this is that, if one generates configuration without taking the number of clusters into account, almost every configuration will be unimportant. A prime example is $n = 0$; the only configurations which matter are the spanning trees, and these are (almost) never generated by occupying links at random. One could also conceive a Monte Carlo algorithm that updates configurations in accordance with the partition function (1.1). Such an algorithm will be difficult to implement, however, because we have long-range interactions, in the sense that the change in the number of clusters by breaking one particular bond may depend on whether some distant bond is occupied. Another disadvantage of these types of Monte Carlo simulations is that they would only generate the correct statistics for one particular n in each run, while the PSRG approach with exact cells only calculates the number of configurations with b bonds and c clusters once, and then profits from this work for each n.

In conclusion, the PSRG approach outlined in this paper is not yet particularly well suited for quantitative numerical calculations of critical exponents. Its value lies rather on a semi-quantitative and conceptual plane. Approximate exponents and RG flows can be calculated with reasonable effort. Also, the identification of the magnetic scaling power with the fractal dimensionality of the percolating cluster suggests a new way to calculate it, investigated in this paper.

References

Aharony A and Stauffer D 1984 *Phys. Rev. Lett.* **52** 2368
Alexander S and Orbach R 1982 *J. Physique* **43** L625
Amit D J 1976 *J. Phys. A: Math. Gen.* **9** 1441
Andelman D and Berker A N 1981 *J. Phys. A: Math. Gen.* **14** L91
Coniglio A 1982 *J. Phys. A: Math. Gen.* **15** 3829
Coniglio A and Klein W 1980 *J. Phys. A: Math. Gen.* **13** 2775
den Nijs M P M 1979 *J. Phys. A: Math. Gen.* **12** 1857
Derrida B and de Sèze L 1982 *J. Physique* **43** 475
Kasteleyn P W and Fortuin C M 1969 *J. Phys. Soc. Japan* **26** *Suppl.* 11
Kadanoff L 1976 *Ann. Phys., NY* **100** 359
Kirkpatrick S 1978 *AIP Conf. Proc.* **40** 99
Mandelbrot B B 1982 *The Fractal Geometry of Nature* (San Francisco: Freeman)
Migdal A A 1976 *Sov. Phys.-JETP* **41** 743
Priest R G and Lubensky T C 1976 *Phys. Rev.* B **13** 4159
Reynolds P J, Klein W and Stanley H E 1977 *J. Phys. C: Solid State Phys.* **10** L167
Reynolds P J, Stanley H E and Klein W 1978 *J. Phys. A: Math. Gen.* **11** L199
Stanley H E 1977 *J. Phys. A: Math. Gen.* **10** L211
—— 1984 *J. Stat. Phys.* **36** 843
Stanley H E and Coniglio A 1983 *Percolation Structures and Processes* (*Ann. Israel Phys. Soc.* vol 5) ed G Deutscher, R Zallen and J Adler (Bristol: Adam Hilger) p 101
Stanley H E, Reynolds P J, Redner S and Family F 1982 *Real-Space Renormalization* ed T W Burkhardt and J M J van Leeuwan (Berlin: Springer)
Wu F Y 1982 *Rev. Mod. Phys.* **54** 235